Experiments to Explore the Influence of Pulse Shaping at the National Ignition Facility

C. A. Thomas,[1] K. L. Baker,[2] D. T. Casey,[2] M. Hohenberger,[2] A. L. Kritcher,[2] B. K. Spears,[2] S. F. Khan,[2] R. Nora,[2] D. T. Woods,[2] J. L. Milovich,[2] R. L. Berger,[2] D. Strozzi,[2] D. D. Ho,[2] D. Clark,[2] B. Bachmann,[2] L. R. Benedetti,[2] R. Bionta,[2] P. M. Celliers,[2] D. N. Fittinghoff,[2] G. Grim,[2] R. Hatarik,[2] N. Izumi,[2] G. Kyrala,[2] T. Ma,[2] M. Millot,[2] S. R. Nagel,[2] C. Yeamans,[2] A. Nikroo,[2] M. Tabak,[2] M. Gatu Johnson,[3] P. L. Volegov,[4] S. M. Finnegan,[4] and E. M. Campbell[1]

[1]Laboratory for Laser Energetics, University of Rochester
[2]Lawrence Livermore National Laboratory
[3]Massachusetts Institute of Technology
[4]Los Alamos National Laboratory

A primary goal of the National Ignition Facility (NIF) is to determine the laser and target requirements for thermonuclear ignition and propagating burn.[1] From detailed numerical simulations and theory, implosion performance should depend on the shape of the laser pulse and the design adiabat α_v of the DT fusion fuel.[2,3] By convention, α_v is the pressure in the cold fuel relative to Fermi-degenerate DT at the maximum velocity of the implosion.[4] In the absence of mechanisms that disturb the fuel, such as preheat, the laser pulse should determine compressibility, and the terms "pulse shaping" and adiabat can be interchangeable. So far, experiments on the NIF have primarily reported tests at $\alpha_v = 1.5$ (Refs. 5 and 6) and $\alpha_v = 2$ to 2.5 (Refs. 7–9) using indirect drive. The integrated performance has improved as issues with hot-spot mix,[10] and target engineering features[11,12] have been identified and mitigated. Changes in the pulse shape may also have played a role but have not been as easy to study. In part, this is because uncertainties in hohlraum and capsule physics complicate the interpretation of simple tests.[13] Existing pulse shapes are also calculated to be at (or near) local optima, making it difficult to motivate new concepts.

To provide new insight, this summary takes advantage of the "BigFoot" platform that was developed to facilitate single-variable studies.[14] This design uses conservative features that are to reduce the number of mechanisms that impact data. As shown in prior work,[15] the yield is a simple and expected function of laser energy per unit target mass, size/scale, and implosion symmetry and shows little to no sensitivity to target quality. These properties simplify the interpretation of data and reduce the number of experiments needed to study changes in pulse shape. As a consequence, we have used this platform to do implosions at two different design adiabats ($\alpha_v = 4$ and 3 ± 0.1) for comparison to calculations, finding that yield and areal density can decrease when adiabat is reduced. Our findings suggest that the optimum design adiabat is presently above 3 and one or more aspects of simulation are incomplete. We have not been able to explain these results in high-resolution calculations using known details of the targets or facility. This study also provides the first direct evidence that performance can increase with compression, although it may be necessary to correct physics that are still unknown to make significant progress.

For background, we briefly explain features of the BigFoot design that make it useful for this work [see Fig. 1(a)]. First, the length of the laser pulse is shorter (and the radius of the hohlraum entrance hole is larger) than calculations suggest is needed for a higher-performing implosion. This reduces the energy coupled to the target (and the expected yield) but makes it easier to control implosion symmetry if changes are made to the laser pulse. Second, BigFoot experiments have minimal laser–plasma instabilities and show no evidence of energetic electrons. This remains true even when changes are made in the length, power, or energy of the laser pulse.[16] Third, the first shock in the ablator/DT is also considerably stronger (≥12 Mbar) than should be necessary for hydrodynamic stability. This reduces the maximum-possible compression of the DT fuel in calculations, but it also limits instabilities seeded by target flaws and imperfections (e.g., the capsule support and fill tube). Fourth, calculations in

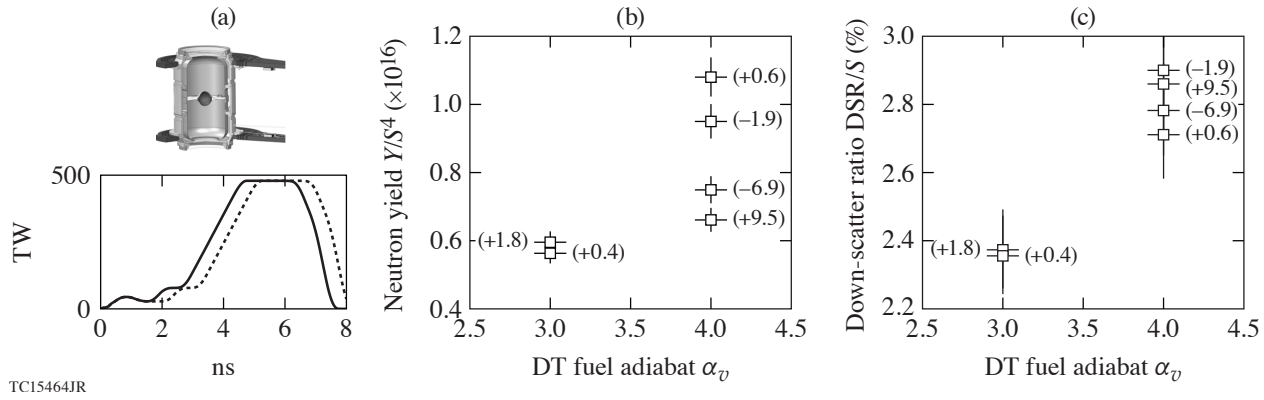

Figure 1
(a) The BigFoot target and laser pulse at $\alpha_v = 4$ (3) are shown by the solid (dashed) line. We also show (b) yield and (c) neutron down-scatter ratio (DSR) normalizing for small changes in target size/scale for six experiments that can be directly compared. The implosion velocity for each is 430±10 km/s. For reference we provide the shape of the hot spot in Legendre P_2 in microns (in parentheses). The yield is correlated to the amplitude of P_2; DSR is not.

LASNEX[17] are able to predict the time of peak emission (±100 ps) and implosion symmetry (±5 μm in P_2) using the measured laser pulse.[18,19] Together, these features make it possible to quickly demonstrate symmetric implosions at different conditions[20] with changes to the laser pulse[21] and to study performance as a function of adiabat.

This summary reports the result of two experiments where the length of the foot (the lower-power section of the laser pulse) is increased by approximately 400 ps, as shown in Fig. 1(a). According to 2-D integrated calculations in *LASNEX*, this should lower the mass-average adiabat of the cold DT fuel from $\alpha_v = 4$ to 3±0.1, increase the DT density at peak implosion velocity, and increase the final neutron yield and DT areal density by factors of 2.9 and 1.15, respectively. We also increased the laser cone fraction (the power on the inner laser cones of the NIF divided by the total) by 3%. Consistent with calculations and prior experiments, these changes reduce the adiabat of the DT but keep other important variables constant, such as the implosion velocity and symmetry.[21] (The shocks launched at each rise in the laser pulse are made to overtake closer to the inner radius of DT ice rather than the DT–ablator interface.) In Fig. 1(b), we show the primary neutron yield Y, as measured at 13 to 15 MeV, and in Fig. 1(c), the neutron–down-scatter ratio (DSR) averaged across multiple measurements. The DSR is a function of neutron emission at 10 to 12 MeV and can be related to the burn-averaged DT areal density (in g/cm^2) as $\rho R_b = 20$ DSR (Ref. 6). [The DSR is averaged over all lines of sight since (1) most implosions are close to symmetric (consistent with imaging data), and (2) diagnostics with a similar line of sight can vary by more than the uncertainty in each.] In contrast to calculations, we find the yield and DSR are reduced at a lower adiabat. Figure 2 addresses the statistical significance of these results. Here, we show a fit to prior BigFoot data at $\alpha_v = 4$ that agrees with the measured yield to ±9% (Ref. 15) and predict the new data in the same way. We find the experiments at lower adiabat are below trend by 40% to 50%, or 4 to 5σ (40% to 9% ≈ 4). It is not possible to explain these results by normal shot-to-shot variations. The yield and DSR at $\alpha_v = 3$ are even below prior data at $\alpha_v = 4$ using smaller capsules at reduced laser energy.

We can illustrate the principles involved with simple models. It is necessary to only assume that the mass forming the hot spot (1) has an initial energy $\sim v^2$ before compression by the cold fuel (it reaches the same implosion velocity as the shell prior to stagnation), (2) is compressed adiabatically with $\gamma = 5/3$ (losses relative to peak compression are small), and (3) achieves a peak radial compression ratio $C_p \sim (v^2/\alpha_v)^{1/2}$ (Ref. 22). If so, the energy in the hot spot $E_h \sim v^2 C_p^2 \sim v^4 \alpha_v^{-1}$. If we also assume that $Y \sim E_h^2$, consistent with $\langle \sigma v \rangle$ at 5 keV (Ref. 23), then $Y \sim v^8 \alpha_v^{-2}$ without accounting for details in hot-spot physics that are uncertain. Since the kinetic energy of the shell is roughly proportional to laser energy E, when the coupling between the hohlraum and capsule is fixed, this is roughly comparable to $Y \sim (E/M)^4 (\alpha_v)^{-2}$, where M is the initial mass of the ablator. This derivation has few assumptions, and it clearly outlines the expected relationship between adiabat, compression, and yield. Since areal density $\sim C_p^2$, it follows that DSR $\sim (E/M)(\alpha_v)^{-1}$. We can increase the sophistication of these models and derive exponents that are slightly

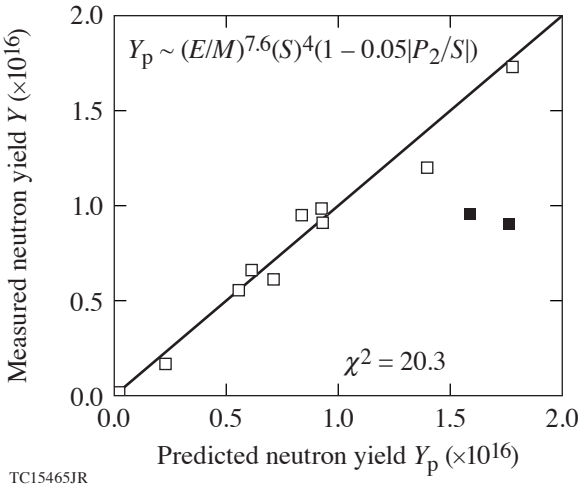

Figure 2
The measured and predicted yield for BigFoot implosions using the analysis in Ref. 15. This model appears to predict data at a design adiabat of 4 (open black squares) but not 3 (solid black squares).

changed (e.g., by including alpha heating, which increases the sensitivity to all terms), but this is not important to interpretation. The yield and DSR should increase together (as shown in Fig. 1) but not by increasing the design adiabat.

To quantify experimental results in the same way, we fit all data to a power law including adiabat and determine the exponents in a least squares sense. For greater accuracy we account for understood changes in laser energy per unit mass (E/M), target size/scale (S), and implosion symmetry (P_2) as in Ref. 15. This exercise is then repeated for DSR with no dependence on P_2 since the data in Fig. 1(c) show no sensitivity. In Fig. 3(a) we assume $Y \sim (E/M)^{N_1}(S)^4(1 - 0.05|P_2/S|)(\alpha_v)^{N_2}$ and find $N_1 = 7.5 \pm 0.3$ and $N_2 = 2.0 \pm 0.1$, for $\chi^2_\nu = 1.2$ (per degree of freedom). In Fig. 3(b) we assume DSR $\sim (E/M)^{N_3}(S)(\alpha_v)^{N_4}$ and find $N_3 = 0.9 \pm 0.2$ and $N_4 = 0.6 \pm 0.1$, for $\chi^2_\nu = 1.1$. These fits are a good representation of data since $\chi^2_\nu \sim 1$, and they behave as expected with the exception of adiabat. In this summary we demonstrate the significance of these findings by fitting the data to subsets of the full model (with no dependence on adiabat) and show that all terms are needed for a good fit. We have proposed to extend this work to a larger range in design adiabat, from 2 to 6. Since these results were unexpected, it is possible that we will find a more-complicated relationship than shown here, with a peak in yield and DSR at a design adiabat other than 4. The value for testing individual aspects of implosion physics is evident, and here, we also discuss the importance of shot-to-shot variability (or reproducibility) to the interpretation of these scalings.

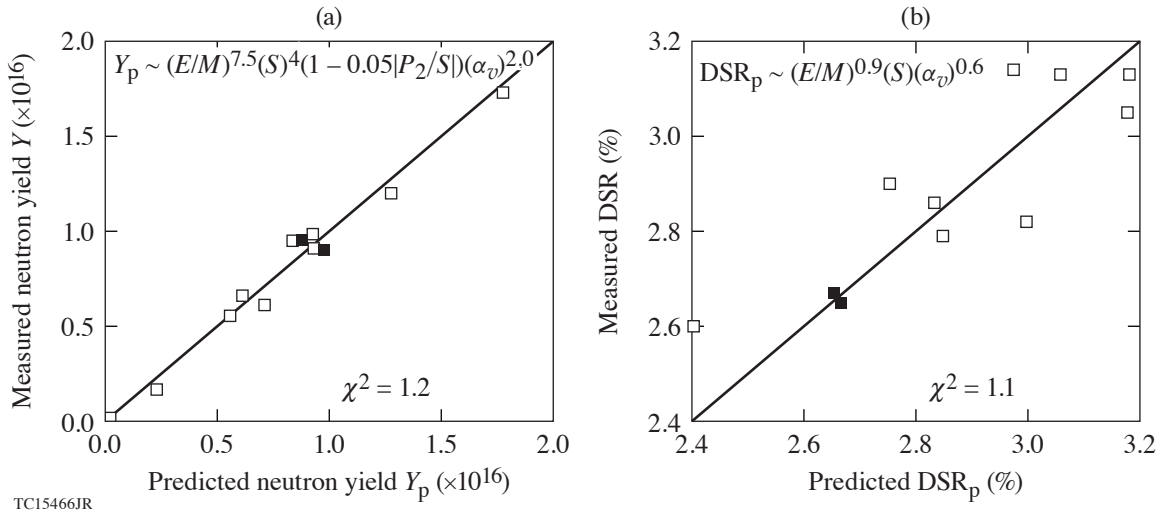

Figure 3
The best model(s) for yield and areal density versus laser energy per unit mass, target scale, hot-spot symmetry, and design adiabat. The residuals are 8.6% and 3.9%, respectively. For reference, we differentiate data at $\alpha_v = 4$ (open black squares) and 3 (solid black squares).

We now examine the peak compression ratio C_p in BigFoot data to check for self-consistency. This quantity is estimated using measurements of the cold fuel since observations of the hot spot (neutron and x-ray imaging) do not have to correlate with pdV work. We begin by defining the areal density at peak compression (without alpha heating) as $\rho R_{p,c} + \rho R_{p,h}$ and at peak burn (with alpha heating) as $\rho R_{b,c} + \rho R_{b,h}$ with contributions from the cold shell and hot spot, respectively. We measure only the latter ρR (typically) but note that alpha heating and electron conduction tend to add energy and mass to the hot spot and reduce the total areal density; as a consequence, $\rho R_{p,c} \geq \rho R_{b,c} + \rho R_{b,h}$. If we then assume that the cold fuel at peak compression has the same mass as the initial DT layer (with areal density $\rho_0 t_0$) and has a relatively thin shell (corrections for a finite hot spot and cold shell are only 1% to 3%), we can put a lower bound on $C_p^2 = \left(\rho R_{b,c} + \rho R_{b,h}\right)/\rho_0 t_0 = 20\ \mathrm{DSR}/\rho_0 t_0$. This formula can be used to compare implosions of different sizes and types when alpha heating is modest $\left(\rho R_{p,h} \ll \rho R_{b,c} + \rho R_{b,h}\right)$ even if hot-spot properties change shot to shot (e.g., due to mix). Figure 4 shows C_p as a function of the mass-averaged first shock velocity in the fusion fuel, u_1, in km/s. This shock is a reasonable surrogate for the design adiabat as described in Ref. 24. Energy deposition should scale as u_1^2, and in simulations we find $\alpha_v \approx 1 + 1.4 \times 10^{-3} u_1^2 - 1.4 \times 10^{-7} u_1^4$ for $u_1 \leq 60$ km/s. The goal of pulse shaping is to maximize compression, so we focus on the upper envelope of data. BigFoot implosions with a mass average $\alpha_v = 4$ ($u_1 \approx 55$ km/s) have a compression ratio of 22 to 23. When BigFoot implosions are performed at a lower adiabat ($\alpha_v = 3$ and $u_1 \approx 40$ km/s) with the same implosion velocity and symmetry, they have a compression ratio of 20 and are more consistent with prior results. We find this analysis can also be used to study compression (relative to expectations) independent of calculations. It is only necessary to decide which data can serve as a reference and project $C_p \sim \alpha_v^{1/2}$. If we assume data at a high adiabat are closer to theory, then this type of extrapolation is given by the solid line in Fig. 4. BigFoot data at $\alpha_v = 3$ appear to be deficient in compression and DSR by 25% and 50%, respectively. Offsets at this level are significant since the laser energy needed to ignite $E_{ign} \sim v^{-6}\alpha_v^2$ (Ref. 25). If $C_p \sim (v^2/\alpha_v)^{1/2}$, this is equivalent to $E_{ign} \sim v^{-2} C_p^{-4} \sim v^{-2}\left(20\ \mathrm{DSR}/\rho_0 t_0\right)^{-2}$. We expect these discrepancies to have an impact on performance and the probability of ignition.

Given these results, we will briefly discuss the mechanisms that could play a role. These could include errors in the strength or timing of shocks.[24] We do not suspect issues of this type because (1) these inferences have been validated using VISAR (velocity interferometer system for any reflector)[26] and (2) we have not identified a systematic error that would cause a U-shaped sensitivity in u_1 (see Fig. 4). It is also possible that we have made an error in the DT equation of state, the stagnation adiabat, or both. Although not presented here, we find that simulations can match the measured yield, temperature, and DSR of BigFoot implosions if they use a higher adiabat than intended by a factor ≥1.4. For capsules that absorb 200 to 250 kJ of x rays, this is equivalent to adding 80 J to the cold DT shell. Simulations would have to underestimate sources of instability, mix at the fuel–ablator interface, or vorticity at small scales.[27] An increase in the effective adiabat could result from residual motion in the cold DT proportional to u_1, which would increase internal energy as u_1^2 after hydrodynamic growth (compression and thermalization). If the ablator were to mix with the DT fuel, this would also increase its absorption of hard x rays. For insight, we will continue to quantify sensitivities in pulse shaping and work to characterize the state of the DT fuel.[28] We also propose to test aspects of stability and,

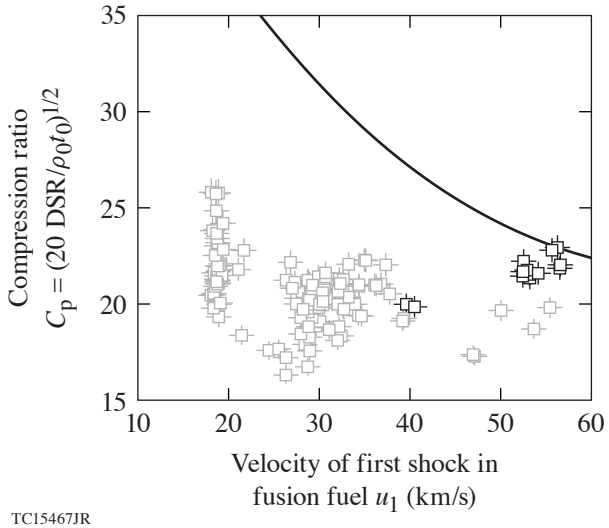

Figure 4
BigFoot data (open black squares) are compared to previous results (open gray squares) on aspects of pulse shaping. Experiments at u_1 of 18, 32, 40, and 55 km/s correspond to α_v of 1.5, 2.3, 3.0, and 4.0, respectively. The solid line is the expected value for a BigFoot-type implosion assuming $C_p \sim \alpha_v^{-1/2}$ at a given velocity and DT mass.

as a start, have made capsules with different levels of high-Z dopant and crystallinity to address hypotheses regarding preheat and microscopic sources of turbulence.[29]

In summary, we have used a platform that is well-suited to single-variable studies to test implosions with different pulse shapes and find $Y \sim (E/M)^{7.5}(S)^4\left(1-0.5\left|P_2/S\right|\right)(\alpha_v)^{2.0}$ and DSR $\sim (E/M)^{0.9}(S)(\alpha_v)^{0.6}$. All terms behave as we expect with the exception of adiabat. These sensitivities will be used to help interpret future work, particularly in circumstances where small or inadvertent changes are made in the laser pulse. If we consider Fig. 4, this could have important implications to compression, and the proximity of ignition. If we only consider the data shown here, a deficit in compression of 25% would be expected to increase the energy needed to ignite by a factor of $1.25^4 \approx 2.4$ relative to expectations.

This work was made possible by the Operations Team at the NIF, target fabrication efforts at General Atomics and LLNL, and the encouragement and support of J. H. Nuckolls, J. D. Lindl, W. L. Kruer, and G. B. Zimmerman. We also thank the Senior Leadership Team at the NIF and note that future communications with the first author should be addressed to the Laboratory for Laser Energetics at the University of Rochester. The data that support the findings of this study are available from the corresponding author upon request. This work was performed under the auspices of the U.S. Department of Energy by Lawrence Livermore National Laboratory under Contract DE-AC52-07NA27344, the Department of Energy National Nuclear Security Administration under Award Number DE-NA0003856, the University of Rochester, and the New York State Energy Research and Development Authority.

1. J. Nuckolls *et al*., Nature **239**, 139 (1972).
2. J. D. Lindl, *Inertial Confinement Fusion: The Quest for Ignition and Energy Gain Using Indirect Drive* (Springer-Verlag, New York, 1998).
3. S. Atzeni and J. Meyer-ter-Vehn, *The Physics of Inertial Fusion: Beam Plasma Interaction, Hydrodynamics, Hot Dense Matter*, 1st ed., International Series of Monographs on Physics, Vol. 125 (Oxford University Press, Oxford, 2004).
4. J. Meyer-ter-Vehn, Nucl. Fusion **22**, 561 (1982).
5. O. L. Landen *et al*., Plasma Phys. Control. Fusion **54**, 124026 (2012).
6. M. J. Edwards *et al*., Phys. Plasmas **20**, 070501 (2013).
7. O. A. Hurricane *et al*., Nature **506**, 343 (2014).
8. D. A. Callahan *et al*., Phys. Plasmas **22**, 056314 (2015).
9. L. F. Berzak Hopkins *et al*., Phys. Rev. Lett. **114**, 175001 (2015).
10. T. Ma *et al*., Phys. Plasmas **24**, 056311 (2017).
11. D. S. Clark *et al*., Phys. Plasmas **23**, 056302 (2016).
12. C. R. Weber *et al*., Phys. Plasmas **24**, 056302 (2017).
13. O. L. Landen *et al*., High Energy Density Phys. **36**, 100755 (2020).
14. K. L. Baker *et al*., Phys. Rev. Lett. **121**, 135001 (2018).
15. C. A. Thomas *et al*., "Principal Factors to Performance in Indirect-Drive Laser Fusion," to be submitted to Physics of Plasmas.
16. R. L. Berger *et al*., Phys. Plasmas **26**, 012709 (2019).

17. G. B. Zimmerman and W. L. Kruer, Comments Plasma Phys. Control. Fusion **2**, 51 (1975).

18. O. S. Jones *et al*., J. Phys.: Conf. Ser. **717**, 012026 (2016).

19. O. S. Jones *et al*., Phys. Plasmas **24**, 056312 (2017).

20. D. T. Casey *et al*., Phys. Plasmas **25**, 056308 (2018).

21. M. Hohenberger *et al*., Phys. Plasmas **26**, 112707 (2019).

22. R. Betti *et al*., Phys. Plasmas **8**, 5257 (2001).

23. R. Betti *et al*., Phys. Rev. Lett. **114**, 255003 (2015).

24. H. F. Robey *et al*., Phys. Plasmas **19**, 042706 (2012).

25. M. C. Herrmann, M. Tabak, and J. D. Lindl, Nucl. Fusion **41**, 99 (2001).

26. H. F. Robey *et al*., Phys. Plasmas **21**, 022703 (2014).

27. B. Cheng *et al*., Plasma Phys. Control. Fusion **60**, 074011 (2018).

28. A. L. Kritcher *et al*., Phys. Rev. Lett. **107**, 015002 (2011).

29. D. D. M. Ho *et al*., J. Phys.: Conf. Ser. **717**, 012023 (2016).